Characterization of a Cylindrical Hall Thruster with Permanent Magnets

IEPC-2011-264

Presented at the 32^{nd} International Electric Propulsion Conference,
Wiesbaden, Germany
September 11–15, 2011

R. Spektor, K. D. Diamant, E.J. Beiting, K. A. Swenson, and D.T. Goddard
The Aerospace Corporation
Y. Raitses and N. J. Fisch
Princeton Plasma Physics Laboratory

Performance and xenon ion laser induced fluorescence measurements of a Cylindrical Hall Thruster with permanent magnets are presented. The thruster produced 3 to 6.5 mN of thrust with a specific impulse between 1000 and 1900 seconds when operated between 200 and 500 V with a xenon anode flow rate between 2.4 to 4.4 sccm. At a discharge potential of 250 V both thrust and specific impulse increased with the anode flow rate. Thruster efficiency also increased with the flow rate. A peak efficiency of 21$\%$ was measured at a flow rate of 3.4 sccm and a discharge voltage near 300 V. The LIF data showed that the plume is less divergent with a magnetic shield. Furthermore, without the shield $\sim 60\%$ of ion acceleration occurred outside of the thruster channel at 250 V, whereas with the shield only 25% of the acceleration occurred outside. Thus, the effect of the magnetic shield is to cause acceleration region to move upstream, similar to overrunning the cathode with a CHT with electromagnets.

I. Introduction

Hall thrusters are not easily amendable to miniaturization. A number of methodologies are available for scaling the thrusters to power levels below a few hundred watts while attempting to preserve specific impulse and efficiency.[1–6] Raitses and Fisch developed 2.6 cm and 3.0 cm diameter Cylindrical Hall Thrusters (CHTs) that operate near 200 W, featuring a reduced surface-to-volume ratio and unique magnetic topology.[7] The central magnetic pole and inner ceramic of the CHT are shortened to produce an annular region near the anode, which is followed by a cylindrical region. In the fully cylindrical configuration (FCHT) the central magnetic pole is flush with the anode, thus completely eliminating the annular region. Detailed studies of the CHT (including the FCHT) in various magnetic field and cathode configurations were presented previously.[8–14]

The 2.6 cm CHT with permanent magnets (CHTpm) is a variant of the FCHT that uses two axially magnetized cobalt-samarium alloy magnet rings instead of electromagnets. Figure 1 shows a photograph and a schematic of this CHTpm. The magnet rings are incorporated into the thruster magnetic circuit with the same polarity in order to implement a direct (enhanced mirror) configuration.[15] Magnetic field simulations and measurements indicate that the magnetic field topologies produced with permanent magnets and electromagnets are similar only inside the thruster channel. In the vicinity of the channel exit and outside the channel the magnetic circuit with the permanent magnets creates a cusped magnetic field (even in the direct configuration). The effect of the magnetic field topology on the thruster performance was investigated in detail in Ref. 16, where thruster performance in the cusped and the direct magnetic field configurations was studied. In the cusped configuration the two magnet rings have opposite polarity.

Moreover, the magnetic field outside the CHTpm is stronger than outside the CHT with the electromagnet coils. A magnetic shield installed in the CHTpm can significantly reduce the field outside.[15] Figure 1 shows the CHTpm with the magnetic shield. Without the shield the ion current density profile in the plume of the CHTpm is hollow, with a region of reduced density at the centerline. With the shield the current density is peaked at the centerline, indicating a more collimated plume.

In this paper we measure the CHTpm performance and investigate its plume properties using Laser Induced Fluorescence (LIF). In particular, we compare performance and plume properties of the CHTpm for various operating points, with and without the magnetic shield, and with two different cathode locations. Furthermore, we compare the

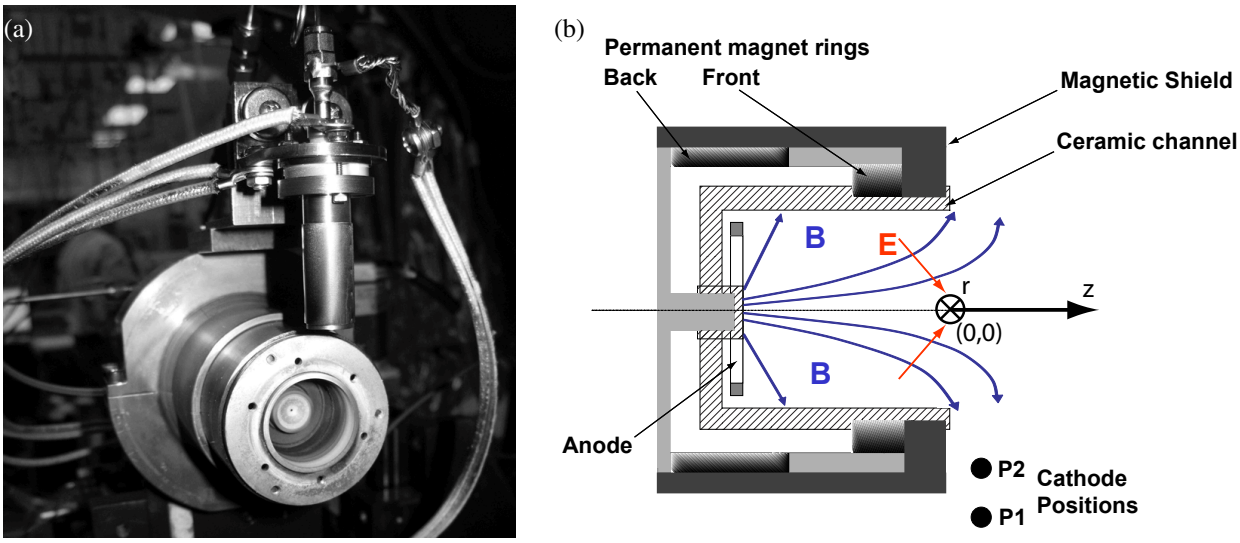

Figure 1. a) Picture of the CHTpm in the Near Field Facility. b) Schematic of the CHTpm with the magnetic shield.

CHTpm (2.6 cm channel diameter) performance with that of the CHTem (3.0 cm channel diameter thruster with electromagnets). A series of thrust measurements at different voltages and flow rates establishes the operating envelope of the thruster, while the LIF technique maps ion velocities in the plume.

The paper is organized conventionally. The thruster configuration and the LIF apparatus are described in Section II. We present and discuss the experimental results in Section III. We conclude by summarizing the pertinent information and suggest avenues for future work in Section IV.

II. Experimental Setup

The experiments were performed in the Near Field Facility (NFF) at The Aerospace Corporation. The facility consists of a 3 m long and 1.5 m diameter stainless steel chamber pumped by two He-cooled nude sails with a maximum pumping speed near 60,000 l/s on Xe. The system has a base pressure of 5×10^{-7} Torr; the pressure increases to as much as 7×10^{-6} Torr (adjusted for Xe) with a thruster operating at 4 sccm to the anode. The pressure was measured with an ionization gauge mounted behind the thruster. A detailed description of the NFF chamber is given in Ref. 17.

The LIF data was collected with the thruster operating at 250 V and 350 V and current between 0.4 and 0.6 A. Two magnetic configurations of the CHTpm were tested – with and without the magnetic shield.[15] For the configuration without the magnetic shield, current of 0.5 A to the cathode keeper was used to keep the thruster operating for more than a few minutes. Two cathode locations were investigated: P1 is 1.0 cm away axially from the thruster exit with the cathode tip 2.35 cm above the channel lip; P2 is at the same axial distance away from the thruster exit as P1 and 1.47 cm from the cathode tip to the upper channel lip. Position P1 is the furthest radial cathode location at which the CHTpm without the magnetic shield could be easily ignited. Position P2 was chosen to minimize the discharge current for the CHTpm with the magnetic shield. A detailed study of the effects of the cathode location can be found in Ref. 18. During the LIF tests reported in the paper the flow rates were nominally 4 and 2 sccm for the anode and cathode respectively. During the performance tests the anode flow rate was varied between 2.4 and 4.4 sccm.

The LIF instrument is designed to measure two-dimensional velocity distribution function profiles of Xe ion and neutral species simultaneously. It is an expanded version of the apparatus previously used to investigate the SPT-140 thruster.[19,20] For this test campaign only the Xe ion velocities were measured. A detailed description of the LIF setup can be found in Ref. 13. The thruster was placed on a motorized platform that could be translated in three orthogonal directions. The data were collected in steps of 0.5 cm in the region from the thruster exit to 4.0 cm along the z (axial) direction, and from the thruster centerline to 3.0 cm along the r (radial) direction, with the thruster exit at the centerline defined as the origin.

Each LIF scan typically covered a frequency range of 40 GHz in 300 data points. Figure 2 displays scans of the axial (panel a) and transverse (panel b) ion velocity distributions at various axial positions and r = 1 cm. These scans were taken with the thruster without the magnetic shield while running at 350 V and the cathode at P2. Each trace in

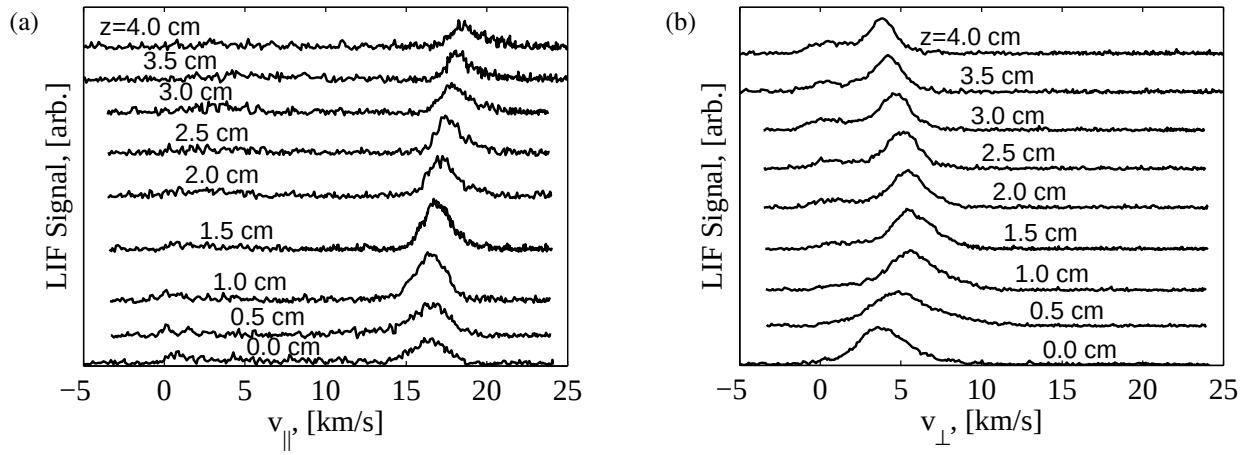

Figure 2. LIF sample data taken at r = 1 cm with the CHTpm (without the magnetic shield) running at 350 V and the cathode in the P2 position. Panel (a) shows the axial component of ion velocity at various locations away from the thruster exit and panel (b) shows the transverse component.

Fig. 2 consists of a single scan, which took around 6 minutes to acquire. At a few locations where the LIF signal-to-noise ratio was low, we collected up to three scans to reduce the measurement uncertainty. The plots in Fig. 2 illustrate that the LIF scans had high signal-to-noise ratios.

Thrust produced by the CHTpm was measured with an inverted pendulum thrust stand employing strain-gauge load cells. The thrust stand is configured as a hinged parallelogram with four aluminum plates and stainless steel shim-stock hinges, which provide little resistance to horizontal motion. Propellant is delivered to the thruster through 1/8 inch diameter stainless steel lines that are secured to the bottom stationary plate, and then bent into a wide corkscrew before attaching to the upper plate on which the thruster is mounted. Electrical power is delivered through bundles of fine-gauge wires that are looped between the plates. The upper plate was placed in contact with the thrust measuring load cell, which was attached to the bottom plate. A second load cell is attached to the upper plate and was used to perform in-situ calibration by applying a load to it and measuring the response of the thrust sensor. This "calibration" sensor takes the place of discrete calibration masses and has the advantage that a continuously variable load can be applied by using a stepper motor to draw up a nylon line attached to it through a spring. Further details on the thrust stand can be found in Ref. 21.

Thrust measurements typically were made by running the thruster to a steady condition, recording the thrust sensor output, shutting the thruster off, and recording the thrust sensor output again. This procedure was repeated at least six times at each operating point. The thrust stand was calibrated after the set of measurements for each operating point. Xenon gas was supplied to the anode and cathode by thermal mass flow controllers, calibrated by timing the pressure rise in a one-liter volume. The cathode flow rate was 2 sccm in all cases. The estimated thrust measurement uncertainty is 5%, determined by combining the average measurement variability with the average uncertainty in the thrust stand calibration. Thrust measurement uncertainty dominated the uncertainties in measured mass flow rate and power, resulting in estimated uncertainties of 5% for anode specific impulse and 10% for anode efficiency. Anode specific impulse I_{sp} and anode efficiency η are defined in the usual manner:

$$I_{sp} = \frac{F}{\dot{m}g} \qquad \text{and} \qquad \eta = \frac{F^2}{2\dot{m}P}, \tag{1}$$

where F is thrust, $\dot{m}$ is the anode mass flow rate, P is thruster input power (main discharge plus keeper), and g is the acceleration due to Earth's gravity at sea level. Figure 3 shows results from operation at anode flow rate of 2.4, 3.4, and 4.4 sccm and discharge voltages from 200 to 500 V. A cathode-keeper discharge was not required to sustain thruster operation, however the effect of running a supplemental keeper discharge at 2.5 A is shown at 250 V. Included on the plots are measurements from Ref. 14 that were taken with the 3 cm CHT thruster operated with electromagnets (CHTem) instead of permanent magnets.

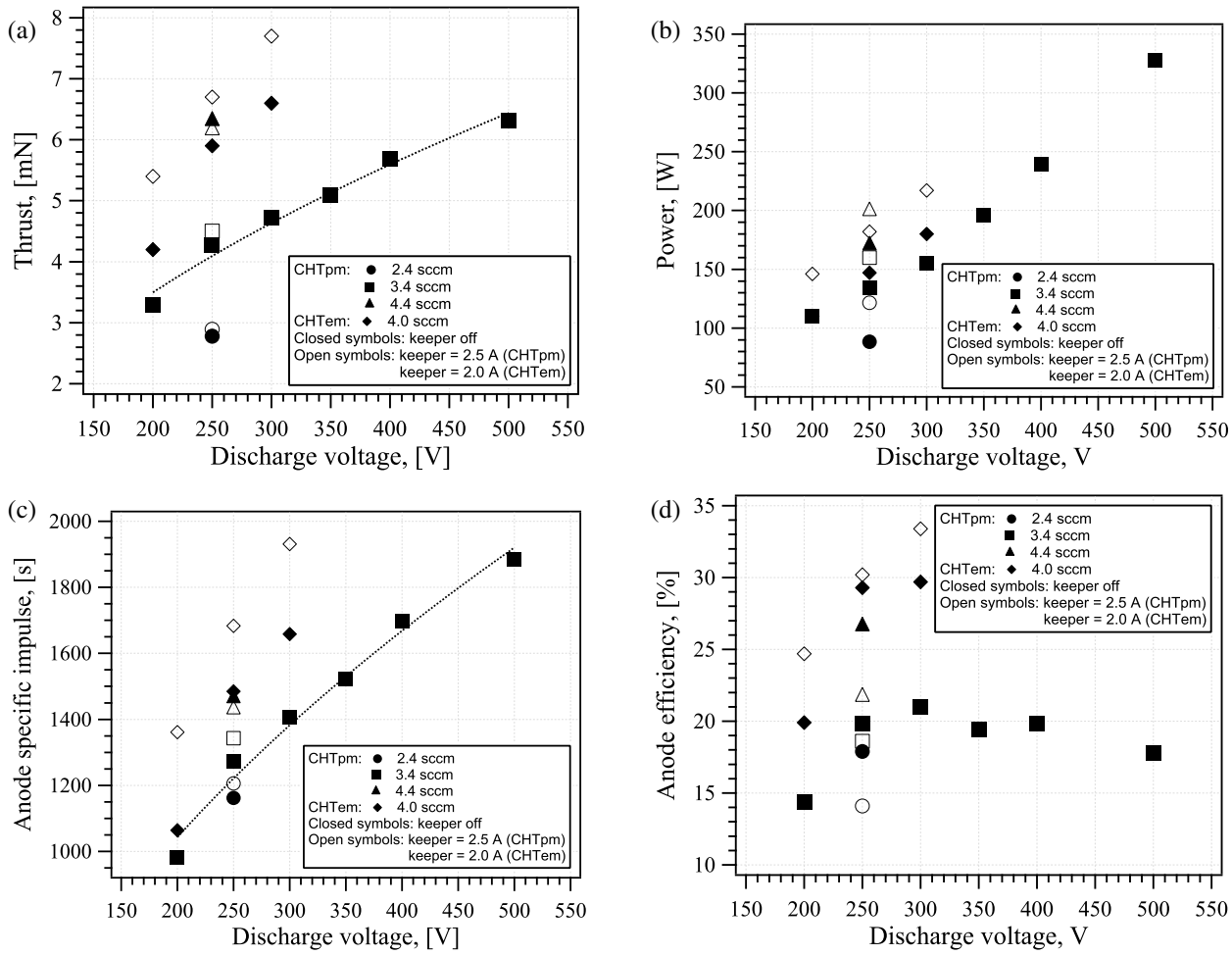

Figure 3. Performance of the CHTpm with the magnetic shield and the cathode in the P2 location. Also, performance of the CHTem (from Ref. 14) is included for comparison. The measurement error for thrust and I_{sp} is 5%, while for efficiency it is 10%. Efficiency calculations include the cathode keeper power but not the electromagnet power.

III. Results and Discussion

Figure 3 shows thruster performance as a function of flow rate and discharge voltage. The CHTpm was operated with the magnetic shield and cathode in the P2 position. The closed symbols indicate thruster operation with the keeper off, while the open symbols indicate that current was drawn to the keeper (2.5 A for CHTpm and 2.0 A for CHTem). We performed the voltage dependence study (200–500 V) with the anode flow rate set at 3.4 sccm, which corresponded to power levels of roughly 100 to 350 W.

In Fig. 3 we see the expected dependencies. Both thrust and specific impulse scaled with the square root of voltage (a fit is shown by the dashed lines). Thrust varied from 3 to 6.5 mN with the flow rate of 3.4 sccm, while the I_{sp} increased from 1000 to over 1800 s as we changed the discharge voltage from 200 to 500 V. The LIF data in Fig. 5 shows an ultimate centerline velocity at 250 V of 17 km/s in this thruster configuration, indicating significant plume divergence ($I_{sp} \sim 1300$ s), low propellant utilization efficiency, or lower velocities off centerline. In our previous studies we found that the centerline exhaust velocity of the CHTem at 250 V in the overrun mode (supplying excess current to the cathode keeper) is approximately 16 km/s with the $I_{sp} \sim 1700$ s, indicating a much smaller ion flux divergence and potentially significant fraction of doubly charged ions, which results in the I_{sp} being larger than the centerline velocity as was found in Ref. 14.

Without a keeper discharge (non-overrun mode), CHTem performance at 250 V and 4 sccm is nearly the same (to within measurement uncertainty) as that of the CHTpm at 250 V and 4.4 sccm. With a keeper discharge (overrun mode) the CHTem performs better than the CHTpm (at 250 V and 4 sccm), particularly with regard to efficiency. The

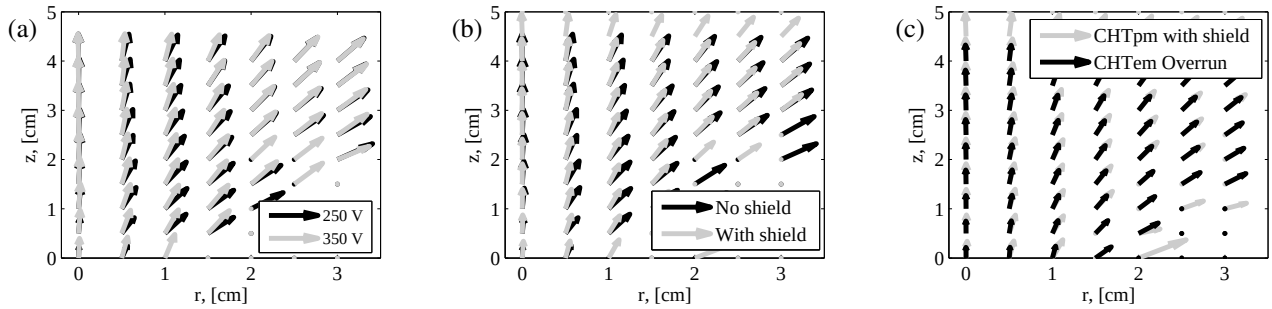

Figure 4. Velocity vector maps: a) No magnetic shield and cathode in the P2 position, b) 250 V and the cathode in the P2 position, c) CHTem in the "Overrun" mode (from Ref. 13) vs. CHTpm with magnetic shield and cathode in the P2 position, both at 250 V. Note: thruster exit is at r = 1.3 cm.

CHTpm efficiency peaks around 300 V at just over 20%. The CHTpm efficiency reported in Ref. 22 is greater than the numbers reported here. While the source of the discrepancy is not clear, the discharge current reported in Ref. 22 is 50% higher than ours as well as that reported in Ref. 18. Thus, there is very likely a significant difference in the reported thruster operation.

We note that even though the CHTem efficiency is 1.5 times higher at a given voltage, this efficiency does not take into account the electro-magnet power consumption, which is around 50 W – as much as a third of the thruster power consumption. If we include the power consumed by the magnets, CHTpm efficiency is higher than that of CHTem. Furthermore, we made only a rudimentary attempt to optimize the magnetic field of the CHTpm and we expect that efficiency can be improved.

Additionally, we investigated the thruster performance as a function of the anode flow rate at 250 V. Thruster efficiency increases to 27%, specific impulse goes up to around 1,600 s, and thrust to ∼6.5 mN, when the flow rate is increased from 3.4 sccm to 4.4 sccm. Unlike the CHTem, we saw no significant difference in the thruster performance with the cathode keeper drawing a current.

Figure 2 shows sample LIF data measured at r = 1 cm and various z (axial) locations with the CHTpm thruster (without magnetic shield) running at 350 V and the cathode at the P1 position. Here the thruster centerline exit location is (0,0) with the thrust axis along the z-axis. The left panel of the figure shows ion acceleration from about 15 km/s to about 20 km/s along the thrust axis as well as a possible slow ion population due to CEX around 0 km/s close to the thruster exit (z between 0 and 1.5 cm). Figures 6-10 in the Appendix show the raw LIF data for all tested conditions. In those figures the bottom traces correspond to z = 0 cm, with each upper trace 0.5 cm further away from the thruster exit. These figures show more indication of the potential charge exchange collisions taking place at the thruster exit. In particular this can be seen from the middle left panel in Fig. 6, in the bottom four panels of Fig. 7, and in the middle left panel of Fig. 8.

We determined the mean ion velocity vector at each measured position in the thruster plume by taking the first velocity moment over the measured LIF trace as described in Ref. 23. This procedure allowed us to create velocity vector maps shown in Fig. 4. We should not interpret such maps as the plume divergence since the LIF measurements do not provide plasma density information, which is needed in addition to the velocity vectors to compute the ion flux.

Although good for qualitative comparison only, the velocity vector maps serve to point out differences and similarities between the various operating regimes of the CHTpm as well as differences from the CHTem thruster. For example, Fig. 4(a) compares the velocity vectors of the CHTpm operated at two different voltages without the magnetic shield and with the cathode in the P2 position. Note that the higher voltage (350 V) results in a more collimated velocity profile. This can be contrasted with a similar study of the CHTpm with the magnetic shield and the cathode in the P1 position (not shown in Fig. 4), where there is no observable difference in the velocity divergence between 250 V and 350 V. These velocity maps are also similar to the ones produced with the thruster without the magnetic shield operated at 350 V and the thruster with the magnetic shield operated at 250 V, both with the cathode at the P2 position. Thus, velocity divergence can be decreased either by the magnetic shield or by increasing the discharge voltage.

It was reported in Ref. 15 that the ion flux profiles are significantly different with and without the magnet shield. Without the shield the ion flux has a hollow profile with two peaks around 50 degrees and a valley at the centerline. On the other hand, with the magnetic shield, ion flux intensity resembles the expected bell-shaped curve. When we compare the velocity vectors of the CHTpm with and without the magnetic shield, as shown in Fig. 4(b), we observe a slightly smaller divergence with the magnetic shield. However, the LIF data does not point to any obvious differences that may help in explaining the hollow shape of the thruster plume without the magnetic shield. This similarity in

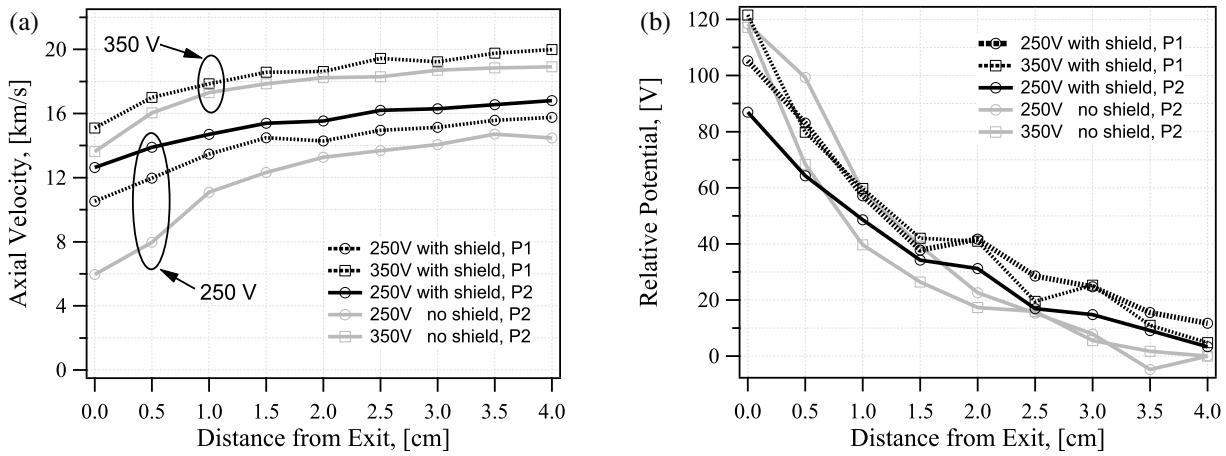

Figure 5. Centerline profiles (r = 0 cm). Panel (a) shows velocity profiles, while panel (b) shows relative potential profiles calculated from panel (a).

the LIF data indicates that the location of the ion production region may be different with and without the magnetic shield. One potential explanation is that the combination of the electric and magnetic fields in the CHTpm without the shield creates an electron density region with a hollow profile. Another potential explanation is that the hollow shape emerges downstream of the measured LIF region (past 4 cm). More analysis is required to understand that plume feature.

In Fig. 4(c) we compare the CHTpm ion velocity divergence in the plume to that of the CHTem thruster. Here we chose the CHTpm configuration with the magnetic shield and the cathode in the P2 position and the CHTem operating in the overrun mode, both running at 250 V. These are the two best configurations for the comparison and we notice no significant difference in the velocity divergence. This is consistent with the findings in Ref. 18, which shows that ion fluxes of the CHTpm with the shield and CHTem in the overrun mode are similar.

Figure 5(a) shows the centerline axial velocity profiles of the CHTpm for the five tested cases. The top two curves correspond to the thruster operating at 350 V while the bottom three curves are for the 250 V cases. The dashed lines indicate thruster operating with the magnetic shield and cathode in the P1 position, while solid lines indicate cathode in the P2 position. At 250 V without the magnetic shield more than half of the ion acceleration ($\sim 60\%$) occurred outside of the thruster. With the shield this fraction dropped to 25%. There was more ion acceleration in the plume (33%) when the cathode was moved from P2 to P1 position. In addition to the ion acceleration moving closer to the anode when the magnetic shield was installed we note an increase in the ultimate exhaust velocity ($v_{||}$ at z = 4 cm). We thus conclude that with the magnetic shield ions are born at a higher potential. This conclusion is consistent with findings reported in Ref. 24.

We can also see the same trend by plotting the electric potentials at the centerline, which is shown in Fig. 5(b). The potentials were computed from the ion centerline axial velocity assuming that the zero potential is at z = 4 cm. Here we see that at 250 V the exit potential of the thruster with the shield was around 90 V, while it was roughly 120 V for the thruster without the shield. Thus, without the shield almost half of the potential drop occurred outside of the thruster channel. Once again, this behavior is similar to overrunning the CHTem where we found that the acceleration region moves inward, closer to the anode, in the overrun configuration when compared to the non-overrun configuration.

IV. Conclusions

In this paper we reported performance and LIF velocity measurements of a miniature Cylindrical Hall Thruster with permanent magnets (CHTpm). Performance measurements were obtained with a magnetic shield installed in the CHTpm and the cathode at the P2 position. We found that in this configuration the thruster produced roughly 3 to 6.5 mN of thrust with the specific impulse between 1000 and 1900 seconds when operating between 200 and 500 V and with the anode flow rate from 2.4 to 4.4 sccm. We found that at 250 V both thrust and specific impulse increased with the anode mass flow rate. Thruster efficiency also increased with the flow rate. At the flow rate of 3.4 sccm the thruster efficiency peaked at just over 20% at a discharge voltage of 300 V. The efficiencies compare favorably to the

CHTem when the power consumed by the electromagnets is included. Optimization of the magnetic field may improve thruster performance.

The LIF data showed that the magnetic shield has a positive effect on the ion velocity divergence profile in the plume. Specifically, there is less divergence when the magnetic shield is installed and the cathode is placed in the P2 position. We also found that ion acceleration region shifts toward the anode with the magnetic shield. Without the shield $\sim 60\%$ of ion acceleration occurs outside of the thruster channel at 250 V. With the shield only 25% of the acceleration occurs outside. Thus, the effect of the magnetic shield on the CHTpm is similar to the effect of overrunning the cathode with the CHTem thruster.

V. Acknowledgements

The project was supported by The Aerospace Corporation through its Independent Research and Development Program.

References

[1]V. Khayms and M. Martinez-Sanchez. Design of a miniaturized Hall thruster for microsatellites. Presented at the 32^{nd} AIAA/ASME/SAE/ASEE Joint Propulsion Conference, Lake Buena Vista, FL, 1-3, July, 1996, AIAA-1996-3291.

[2]V. Hruby, J. Monheiser, B. Pote, P. Rostler, J. Kolencik, and C. Freeman. Development of low power Hall thrusters. Presented at the 30^{th} Plasmadynamics and Lasers Conference, Norfolk, VA, 28 June - 1 July, 1999,AIAA-1999-3534.

[3]N.Z. Warner and M. Martinez-Sanchez. Design and preliminary testing of a miniaturized tal Hall thruster. Presented at the 42^{nd} AIAA/ASME/SAE/ASEE Joint Propulsion Conference (JPC), Sacramento, CA, 9-12 July 2006, AIAA-2006-4994.

[4]F. Battista, E. DeMarco, T. Misuri, and M. Andrenucci. A review of the Hall thruster scaling methodology. Presented at the 30^{th} International Electric Propulsion Conference, Florence, Italy, 17-20 September 2007, IEPC-2007-313.

[5]M. Belikov, O. Gorshkov, E. Dyshlyuk, A. Lovtzov, and A. Shagayda. Development of low-power Hall thruster with lifetime up to 3000 hours. Presented at the 30^{th} International Electric Propulsion Conference, Florence, Italy, 17-20 September 2007, IEPC-2007-129.

[6]E. Ahedo and J Gallardo. Scaling down Hall thrusters. Presented at the 28^{th} International Electric Propulsion Conference, Toulouse, France, 17-20 March 2003, IEPC-2003-104.

[7]Y. Raitses, N.J. Fisch, K.M. Ertmer, and C.A. Burlingame. A study of cylindrical Hall thruster for low power space applications. Presented at the 36^{th} AIAA/ASME/SAE/ASEE Joint Propulsion Conference, Huntsville, AL, July 2000, AIAA-2000-3421.

[8]Y. Raitses and N. J. Fisch. Parametric investigations of a nonconventional Hall thruster. *Phys. Plasmas*, 8(5):2579, May 2001.

[9]A. Smirnov, Y. Raitses, and N. J. Fisch. Plasma measurements in a 100 W cylindrical Hall thruster. *J. Appl. Phys.*, 95(5):2283, March 2004.

[10]Y. Raitses, A. Smirnov, and N.J. Fisch. Enhanced performance of cylindrical Hall thrusters. *Applied Phys. Let.*, 90:221502, 2007.

[11]A. Smirnov, Y. Raitses, and N.J. Fisch. Experimental and theoretical studies of cylindrical Hall thrusters. *Phys. Plasmas*, page 057106, 2007.

[12]R. Spektor, K.D. Diamant, E.J. Beiting, Y. Raitses, and N.J. Fisch. LIF measurements of the Cylindrical Hall Thruster plume. Presented at the 31^{st} International Electric Propulsion Conference (IEPC), Ann Arbor, MI, USA Sep. 20–24, 2009. IEPC-2009-137.

[13]R. Spektor. Laser induced fluorescence measurements of the cylindrical hall thruster plume. *Phys.Plasmas*, 17(093502), 2010.

[14]Y. Raitses K. D. Diamant, J. E. Pollard and N. J. Fisch. Ionization, plume properties, and performance of cylindrical hall thrusters. *IEEE. Trans. Plasma Science*, 38(4), 2010.

[15]Y. Raitses, J. C. Gayoso, E. Merino, and N. J. Fisch. Effect of the magnetic field on the plasma plume of the cylindrical hall thruster with permanent magnets. Presented at the 46^{th} AIAA/ASME/SAE/ASEE Joint Propulsion Conference, Nashville, TN, July 25-28, 2010, AIAA-2010-6621.

[16]K.A. Polzin, E.S. Sooby, A.C. Kimberlin, Y. Raitses, E. Merino, and N. J. Fisch. Performance of a permanent-magnet cylindrical hall-effect thruster. Presented at the 45^{th} AIAA/ASME/SAE/ASEE Joint Propulsion Conference, Nashville, TN, August 2-5, 2009, AIAA-2009-4812.

[17]R. Spektor and E. J. Beiting. Non-invasive plasma diagnostic inside a Hall thruster discharge. Presented at the 30^{th} International Electric Propulsion Conference (IEPC), Florence, Italy Sep. 17–20, 2007. IEPC-2007-69.

[18]J. C. Gayoso, Y. Raitses, and N. J. Fisch. Cathode effects on operation and plasma plume of the permanent magnet cylindrical hall thruster. Presented at the 47^{th} AIAA/ASME/SAE/ASEE Joint Propulsion Conference, San Diego, Ca, June 31 - July 3, 2011, AIAA-2011-5996.

[19]E.J. Beiting and J.E. Pollard. Measurements of xenon ion velocities of the SPT-140 using laser induced fluorescence. Presented at the 3^{rd} International Conference of Spacecraft Propulsion, Cannes, France, October 10–13, 2000.

[20]J.E. Pollard and E.J. Beiting. Ion energy, ion velocity, and thrust vector measurements for the SPT-140 Hall thruster. Presented at the 3^{rd} International Conference of Spacecraft Propulsion, Cannes, France, October 10–13, 2000.

[21]J. E. Pollard and R. P. Welle. Thrust vector measurements with the T5 ion engine. Presented at the 31^{st} AIAA/ASME/SAE/ASEE Joint Propulsion Conference (JPC), San Diego, CA, July 10–12, 1995, AIAA1995-2829.

[22]K.A. Polzin, Y. Raitses, J. C. Gayoso, and N. J. Fisch. Comparisons in performance of electromagnet and permanent-magnet cylindrical hall-effect thrusters. Presented at the 46^{th} AIAA/ASME/SAE/ASEE Joint Propulsion Conference, Nashville, TN, July 25-28, 2010, AIAA-2010-6695.

[23]R. Spektor. Computation of two-dimensional electric field from the ion laser induced fluorescence measurements. *Phys.Plasmas*, 17(093503), 2010.

[24]Y. Raitses, J. C. Gayoso, and N. J. Fisch. Magnetic shielding for plume reduction and suppression of discharge oscillations in the permanent magnet Hall thrusters. Presented at the 32^{nd} International Electric Propulsion Conference, Ann Arbor, Michigan, USA, 10-15 September 2011, IEPC-2011-175.

A. Raw LIF data

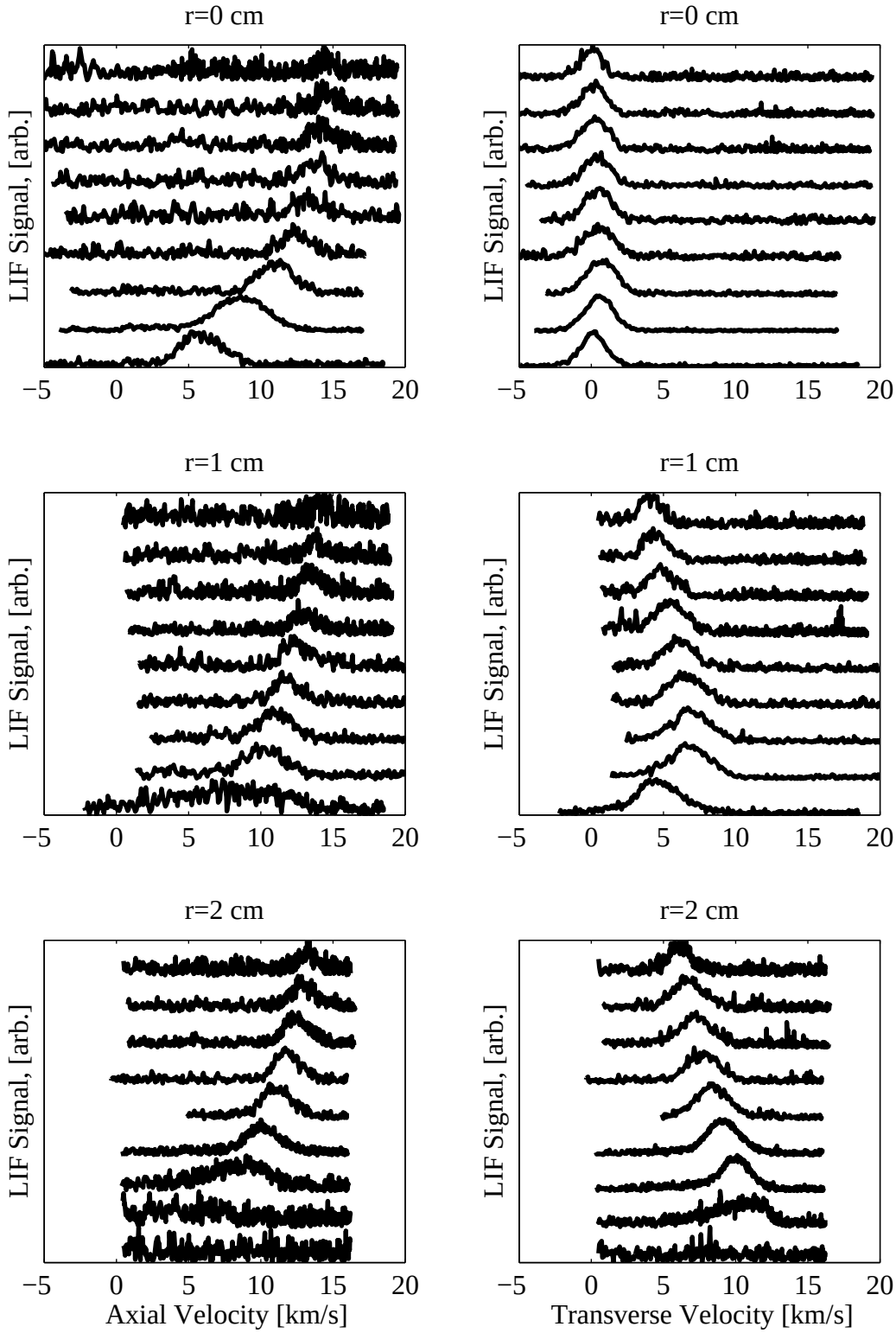

Figure 6. CHTpm without the magnetic shield and with the cathode in the P2 position at 250V

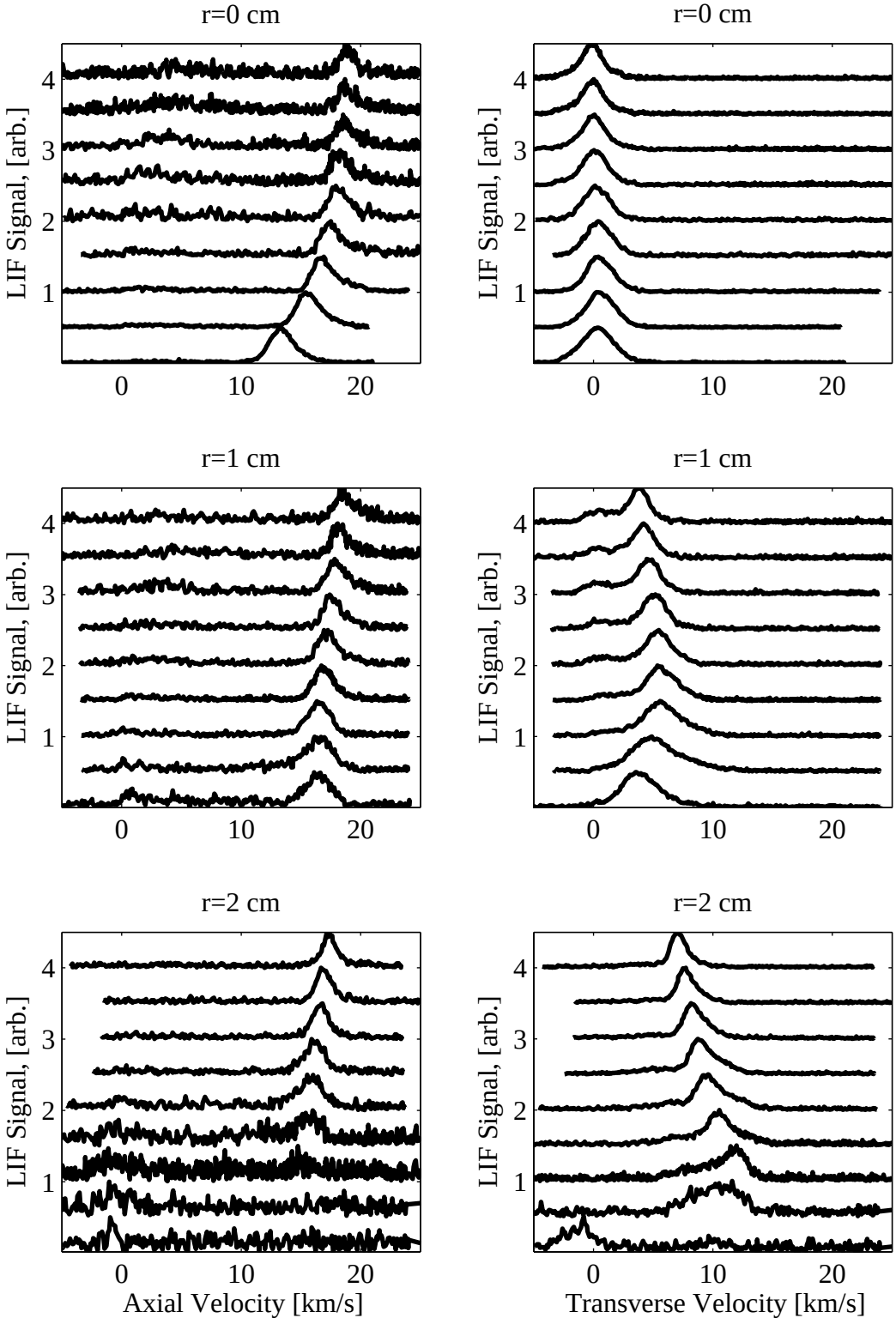

Figure 7. CHTpm without the magnetic shield and with the cathode in the P2 position at 350V

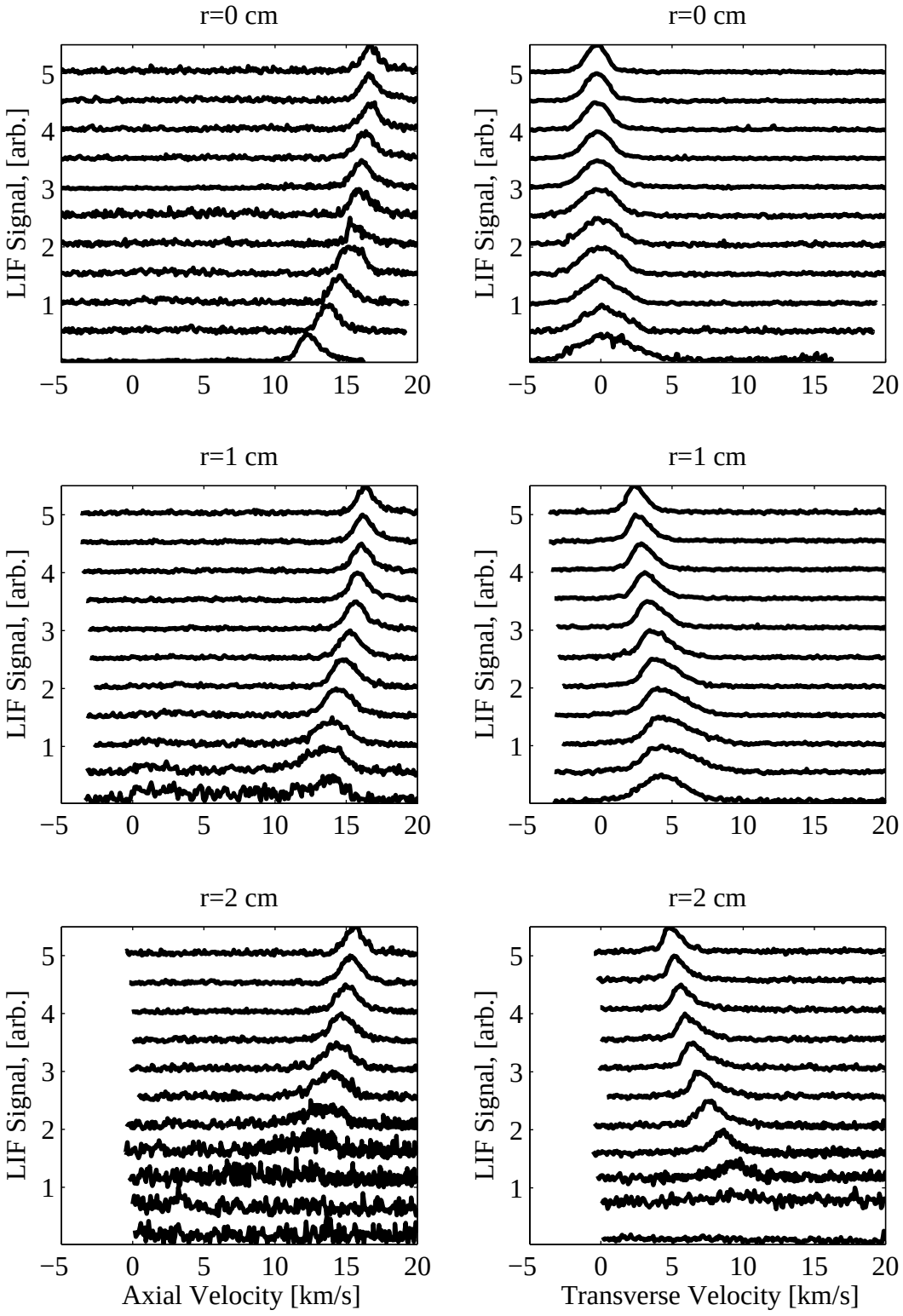

Figure 8. CHTpm with the magnetic shield and with the cathode in the P2 position at 250V

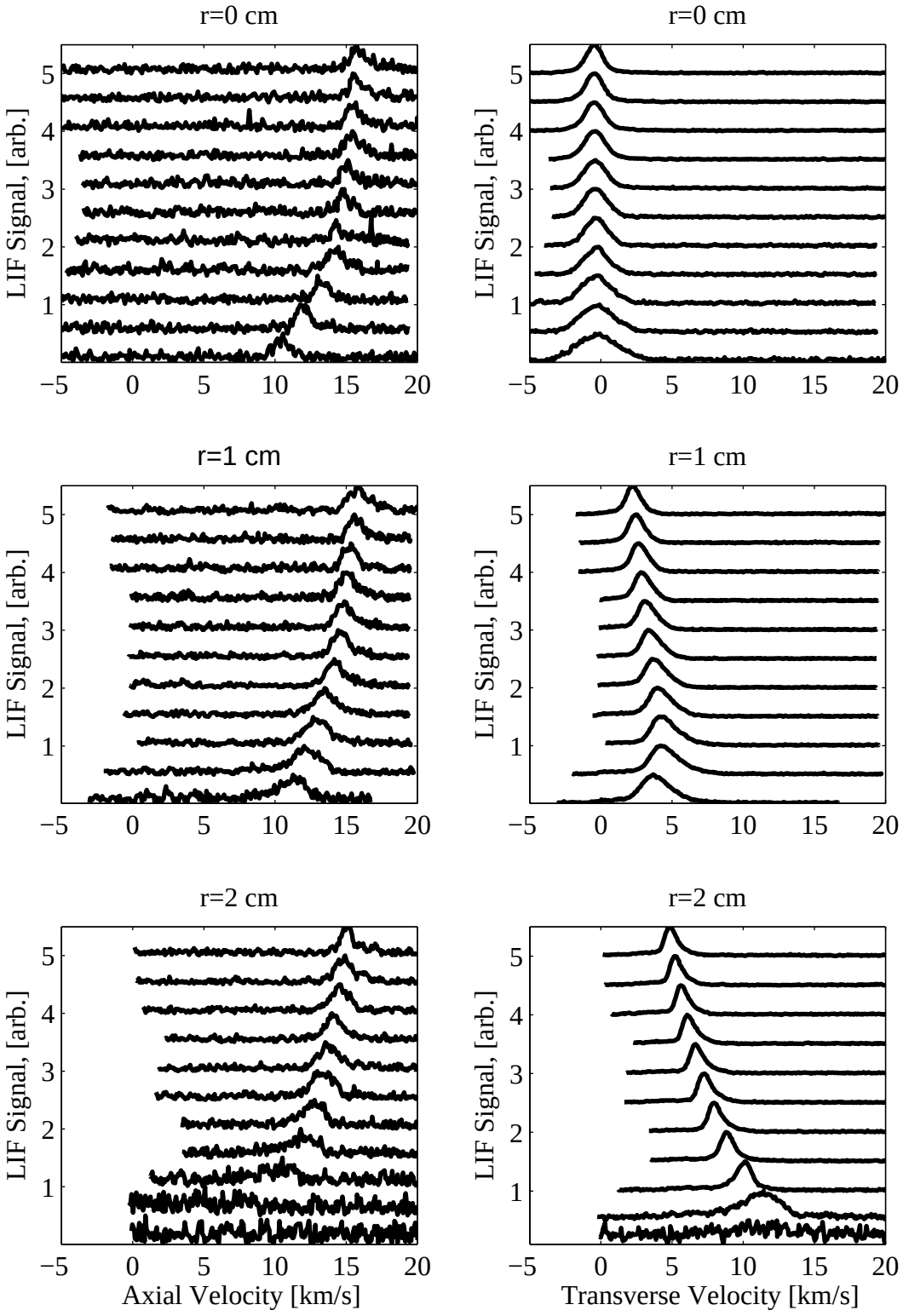

Figure 9. CHTpm with the magnetic shield and with the cathode in the P1 position at 250V

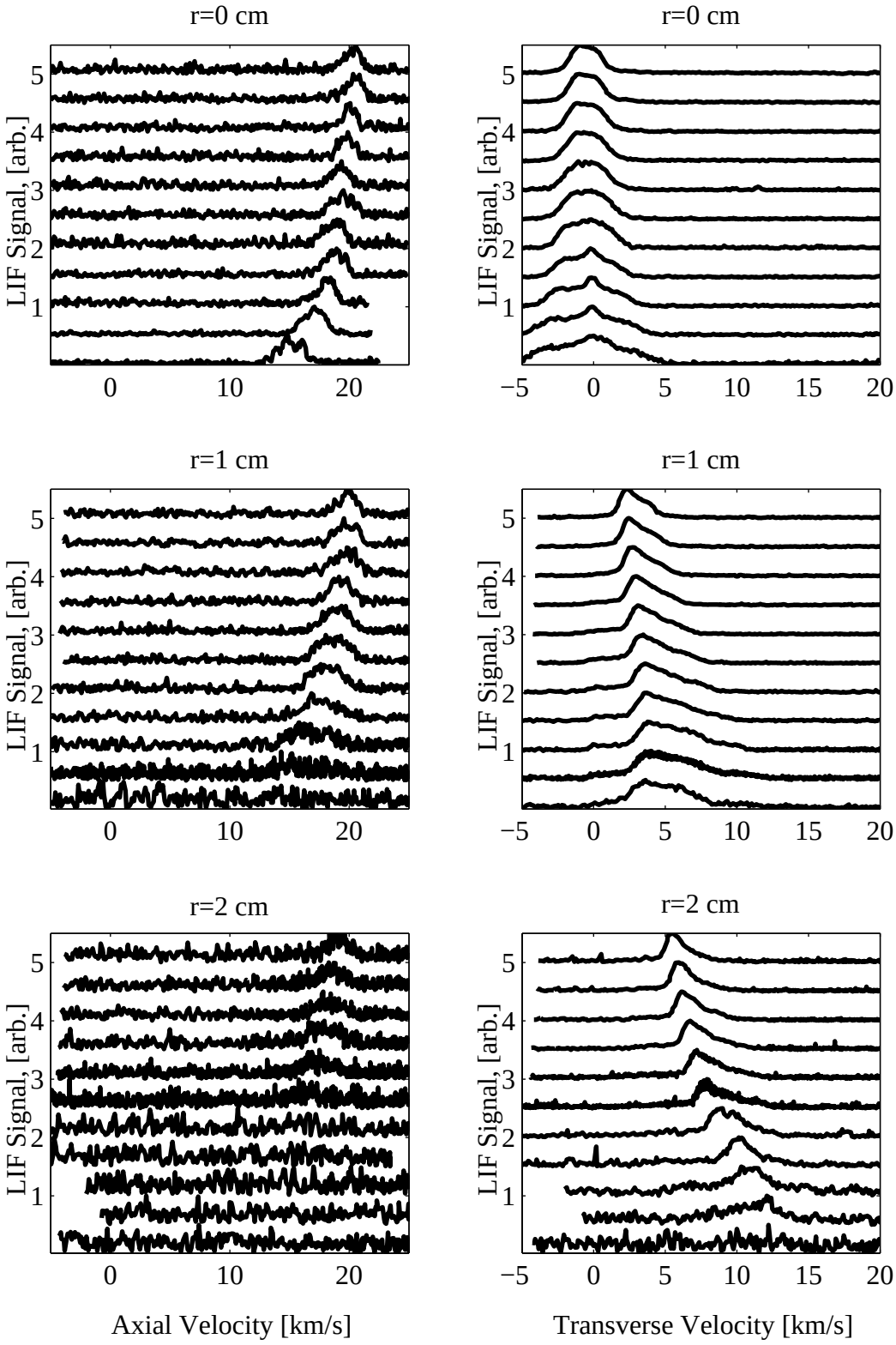

Figure 10. CHTpm with the magnetic shield and with the cathode in the P1 position at 350V